Nanomedicine: Nanotechnology, Biology, and Medicine
20 (2019) 102017

nanomedjournal.com

Delivery of siRNA using folate receptor-targeted pH-sensitive polymeric nanoparticles for rheumatoid arthritis therapy

Xiangshi Sun, MD[a], Shiyan Dong, MD[a], Xiangyu Li, MD[a], Kongtong Yu, PhD[a], Fengying Sun, PhD[a], Robert J. Lee, PhD[a,b], Youxin Li, PhD[a,*], Lesheng Teng, PhD[a,*]

[a]*School of Life Sciences, Jilin University, Changchun, China*
[b]*Division of Pharmaceutics and Pharmaceutical Chemistry, The Ohio State University, Columbus, OH, USA*

Revised 1 May 2019

Abstract

Systemic delivery of siRNA to target tissues is difficult to achieve owing to its limited cellular uptake and poor serum stability. Herein, polymeric nanoparticles were developed for systemic administration of siRNA to inflamed tissues. The polymeric nanoparticles were composed of PK3 as a pH-sensitive polymer, folate-polyethyleneglycol-poly(lactide-co-glycolide) as a targeting ligand, and a DOTAP/siRNA core. The polymeric nanoparticles had a mean particle size of 142.6 ± 0.61 nm and a zeta potential of 3.6 ± 0.43 mV. *In vitro* studies indicated pH-dependent siRNA release from polymeric nanoparticles, with accelerated release at pH 5.0. Cellular uptake was efficient and gene silencing was confirmed by Western blot. *In vivo*, polymeric nanoparticles were shown to have inflammation-targeting activity and potent therapeutic effects in an adjuvant-induced arthritis rat model. These results suggest that pH-sensitive and folate receptor-targeted nanoparticles are a promising drug carrier for siRNA delivery for rheumatoid arthritis.

Keywords: Rheumatoid arthritis; siRNA; PK3; Folate; Nanoparticles

Background

Rheumatoid arthritis (RA) is an autoimmune disease with an incidence of about 1%.[1] Currently, clinical therapy for RA mainly includes nonsteroidal anti-inflammatory drugs (NSAIDs), glucocorticoids (GCs), disease-modifying anti-rheumatic drugs (DMARDs) and biological response modifiers (BRMs).[2] NSAIDs and GCs are used for the alleviation of pain and inflammation of RA.[3,4] Chronic and high-dose use of NSAIDs and GCs may lead to serious side effects.[4,5] DMARDs, slow-acting anti-rheumatic agents, can slow the progression of RA.[6] However, DMARDs have drug resistance and specific toxicity.[7,8] Nevertheless, DMARDs are used for the first-line medication for RA therapy.[9] BRMs are designed to target inflammatory cytokines or pathways for the treatment of RA, becoming the new class of drugs for RA therapy.[10,11]

Although the etiology of RA is still obscure, studies have demonstrated that macrophages are crucial to the pathogenesis of RA.[12] In RA joints, overexpressed pro-inflammatory cytokines, which are mainly released by activated macrophages, cause the inflammation of joint, resulting in cartilage and bone destruction.[13,14] Several mechanisms have been identified that contributed to the avoidance of macrophages apoptosis in RA.[15,16]

Myeloid cell leukemia-1 (Mcl-1), a member of anti-apoptotic B-cell lymphoma-2 (Bcl-2) family, has been found to be overexpressed in macrophages from RA joints.[17] Mcl-1 protects macrophages against apoptosis through preventing the activation of pro-apoptotic molecules Bax, Bak, and Bim.[18] Studies have shown that inhibition of Mcl-1 leads to apoptosis of macrophages, suggesting that Mcl-1 is an important therapeutic target in RA.[18,19] Furthermore, Folate receptor β (FRβ), which is highly expressed on activated macrophages, is a useful biomarker for targeted drug delivery.[20]

Small interfering RNA (siRNA) is able to specifically silence gene expression *via* RNA interference (RNAi).[21] RNAi-based

Abbreviations: PK3, a novel polyketal; FA-PPNPs, nanoparticles composed of FA-PEG-PLGA and PK3; FA-PNPs, nanoparticles composed of FA-PEG-PLGA; FA-siRNA-PPNPs, Mcl-1 siRNA loaded FA-PPNPs; FA-siRNA-PNPs, Mcl-1 siRNA loaded FA-PNPs

This study was supported by Jilin Province Science and Technology Development Program (No. 20180101269JC).

*Corresponding author: School of life sciences, Jilin University, Changchun, China.

E-mail addresses: liyouxin@jlu.edu.cn, (Y. Li), tenglesheng@jlu.edu.cn. (L. Teng).

https://doi.org/10.1016/j.nano.2019.102017
1549-9634/

therapy offers a novel approach for the treatment of RA.[22] However, the clinical application of siRNA is severely hampered by its low delivery efficiency.[23] Due to its high molecular weight, hydrophilicity, and negative charge, an siRNA does not readily enter the cell through passive diffusion.[24] Moreover, siRNA is susceptible to nucleases and has a short half-life in serum.[25] Therefore, a safe and efficient delivery system is vital for clinical application of siRNA.

Polymeric nanoparticles (PNPs) are promising vehicles for systemic siRNA delivery in RA therapy. Nanoparticles are associated with prolonged blood circulation, extravasation through leaky vasculature and subsequent inflammatory cell-mediated sequestration (ELVIS) in inflammatory tissues.[26–28] Cationic polymers and cationic lipids have been applied in PNPs for delivery of siRNA due to their ability to electrostatically complex with the cargo.[29] Among these, 1, 2-dioleyl-3-trimethylammonium propane (DOTAP) is the most widely used cationic lipid, which is biodegradable and has low cytotoxicity.[30]

In order to efficiently deliver drugs to inflamed tissue, pH-sensitive nanoparticles based on polyketal are exploited.[31] PK3, a novel polyketal, has a short hydrolytic half-time and produces neutral degradation products at pH 4.5.[32] PNPs constructed of PK3 have long circulation in the blood and rapid release of drugs in endosomes and lysosomes. Therefore, PK3 is a promising carrier for treatment of inflammatory diseases and cancer.

In this study, we developed a novel polymer nanoparticle (FA-PPNPs) for delivery of Mcl-1 siRNA to inflamed joints in RA. For the synthesis of the nanoparticle, siRNA-cationic lipid complexes were first prepared and then encapsulated in PK3 and folate-polyethyleneglycol-poly(lactide-co-glycolide) (FA-PEG-PLGA). Herein, we evaluated the physicochemical characteristics of Mcl-1 siRNA-loaded FA-PPNPs (FA-siRNA-PPNPs). Moreover, the *in vivo* tissue distribution and therapeutic effect of FA-siRNA-PPNPs were also investigated in adjuvant-induced arthritis (AIA) rat model.

Methods

Materials

FA-PEG-PLGA and PLGA were purchased from Xian Ruixi Biological Technology Co. Ltd. (Xian, China). Mcl-1 siRNA (5′-AAGUAUCACAGACGUUCUCTT-3′, 5′-GAGAACGUCUGUGAUACUUTT-3′), and Cy5-labeled siRNA were purchased from Ribo Biochemistry (Guangzhou, China). 1,2-Dioleoyl-3-trimethylammonium-propane (DOTAP) was obtained from Lipoid (Newark, NJ, USA). Dulbecco's modified Eagle's medium (DMEM) and fetal bovine serum (FBS) were purchased from Procell Biological Technology (Wuhan, China). Polyvinyl alcohol (PVA) (M.W. 13,000–23,000 Da, 87%–89% hydrolyzed) and lipopolysaccharide (LPS), and 4′,6-Diamidino-2-phenylindole (DAPI) were purchased from Sigma-Aldrich (St Louis, MO, USA). 3-(4,5-Dimethylthiazol-2-yl)-2,5-diphenyltetrazolium bromide (MTT) was purchased from Yuanye Biotechnology (Shanghai, China). Diethylpyrocarbonate (DEPC)-treated water was purchased from Beyotime (Beyotime, Haimen, China).

Preparation of FA-siRNA-PPNPs

PK3 were synthesized as described previously.[32] The Bligh and Dyer extraction method was used to synthesize DOTAP/Mcl-1 siRNA complexes.[33] Briefly, 500 μL of DOTAP in dichloromethane (2.5 mg/mL) was added dropwise into 500 μL of Mcl-1 siRNA in DEPC-treated water (4 μM) under sonication. Then, 1.05 mL of methanol was added to form a monophase for 30 min at room temperature. DOTAP/siRNA lipoplexes were extracted into the bottom dichloromethane phase by the addition of dichloromethane and water (500 μL each) under vortex followed by centrifugation at 5000 rpm for 5 min.

The DOTAP/siRNA lipoplexes were encapsulated in FA-PEG-PLGA and PK3 by an emulsion–solvent evaporation method. FA-PEG-PLGA and PK3, dissolved in dichloromethane, were added into the DOTAP/siRNA lipoplexes in dichloromethane; 1 mL of acetone was then added to the dichloromethane solution to form an organic phase. The organic phase was added slowly into 4 mL of 2% (w/v) PVA under sonication followed by continued sonication using a 200 W ultrasonic processor (JY 92-IIN, Scientz, Ningbo, China) for 3 min, and then dispersed in 10 mL of DEPC-treated water. The mixture was stirred for 4 hr. at room temperature to volatilize organic solvent. The resulting FA-siRNA-PPNPs were isolated by centrifugation at 18,000 rpm at 4 °C for 15 min, washed three times with DEPC-treated water, freeze-dried and stored at 4 °C until use. Fluorescently labeled nanoparticles were prepared using the same method, except for the replacement of siRNA with Cy5-labeled siRNA.

Characterization of FA-siRNA-PPNPs

Particle size, polydispersity index (PDI) and zeta potential of PPNPs were determined on a Zetasizer Nano ZS90 (Malvern, UK). The morphology of FA-siRNA-PPNPs was investigated by transmission electron microscopy (TEM) (H-800, Hitachi, Tokyo, Japan).

To determine the percentage of RNA loading and siRNA encapsulation efficiency (EE), Cy5-siRNA was used to prepare nanoparticles. Fluorescence intensity of Cy5 in the supernatant was measured after centrifugation by the fluorescent plate reader (ex/em = 650/670 nm). The percentage of RNA loading and EE were calculated using equations below:

$$\text{RNA loading}\ (\%) = \frac{\text{mass of total siRNA} - \text{mass of siRNA in the supernatant}}{\text{mass of nanoparticles}} \times 100\%\text{EE}\ (\%)$$

$$= \frac{\text{mass of total siRNA} - \text{mass of siRNA in the supernatant}}{\text{mass of total siRNA}} \times 100\%.$$

Stability of PNPs

Lyophilized FA-siRNA-PPNPs were resuspended in deionized water, PBS (10 mM, pH 7.4), or PBS (10 mM, pH 7.4) containing 10% FBS, and incubated at 37 °C or 4 °C. Change in the particle size was determined daily to evaluate the colloidal stability of FA-siRNA-PPNPs. The zeta potential of FA-siRNA-

PPNPs in different media were determined after centrifugation and resuspending in deionized water. The siRNA encapsulation efficiency of FA-siRNA-PPNPs was also determined. The morphology of FA-siRNA-PPNPs were determined by TEM after 7 days' incubation.

In vitro release

The release of siRNA from FA-siRNA-PPNPs was measured using fluorescently labeled Cy5-siRNA-loaded nanoparticles. FA-siRNA-PPNPs were suspended in the buffer of pH 7.4 and pH 5.0 to simulate the neutral physiological condition and acidic intercellular microenvironment in the endosomes (pH 5.0–6.0) and lysosomes (pH 4.0–5.0).[34] To evaluate the pH-sensitive release profiles, 1 mL of FA-siRNA-PPNPs in PBS (10 mM, pH 7.4 or 5.0) was transferred in a dialysis bag of MWCO 50 kDa, which was placed in 20 mL PBS (10 mM, pH 7.4 or 5.0) in a shaker incubator operating at 100 rpm and 37 °C. 1 mL of the release medium was collected at intervals, while the same volume of fresh PBS was added into the release medium. The concentration of released siRNA was measured by its fluorescence intensity.

Hemolysis assay

To evaluate the hemocompatibility of PNPs, hemolysis by the nanoparticles was investigated. Rat blood sample was collected and centrifuged to separate the red blood cells (RBCs). RBCs were washed and dispersed in 50 volume of saline and incubated with FA-siRNA-PPNPs or FA-siRNA-PNPs at a concentration of nanoparticles from 3.1 to 100 μg/mL for 30 min at 37 °C. RBCs treated with the same volume of Triton-X and saline were set as positive and negative controls. Then, the absorbance of supernatants was measured at 540 nm after intact RBCs removed by centrifugation. The percentage of hemolysis was calculated using the equation below.

$$\text{Hemolysis}\ (\%) = \frac{\text{Asample}-\text{Anegative control}}{\text{Apositive control}-\text{Anegative control}} \times 100\%$$

where A_{sample} represented the absorbance of the sample treated with nanoparticles, $A_{positive\ control}$ represented sample treated with Triton-X, and $A_{negative\ control}$ represented sample treated with saline.

Cell culture

RAW 264.7 cells were cultured in DMEM containing 10% FBS at 37 °C in a humidified atmosphere containing 5% CO_2. For the cellular study, RAW 264.7 cells were activated by 1 μg/mL LPS for 48 h.

Cell-uptake studies

Activated RAW 264.7 cells were seeded in 6-well plate (2×10^5 cells/well) and incubated overnight. Then, FA-siRNA-PPNPs or FA-siRNA-PNPs formulated with Cy5-siRNA (100 nM) in DMEM were applied and incubated for 4 hr. Untreated cells and cells treated with the same concentration of naked Cy5-siRNA were also investigated at the same condition. After washing with PBS three times, 1 mL of 4% (w/v) paraformaldehyde solution was added into each well to fix cells for 15 min. The fluorescence intensity of cells was investigated on a flow cytometer (BD Biosciences, San Jose, CA, USA).

Intracellular distribution of PNPs

Activated RAW 264.7 cells containing FA-siRNA-PPNPs and FA-siRNA-PNPs loaded with Cy5-siRNA (100 nM) were cultured in a 12-well plate (1×10^5 cells/well) on a coverslip for 4 hr. After washing with PBS three times, cells were fixed with 4% (w/v) paraformaldehyde solution for 15 min. Then, 100 μL of DAPI (5 μg/μL) was added and incubated for 3 min. The cells were visualized using an LSM710 confocal laser scanning microscopy (CLSM) (Carl Zeiss, Jena, Germany).

Cytotoxicity assays

Cytotoxicity of nanoparticles was investigated by MTT assay. Activated RAW 264.7 cells were cultured in a 96-well plate (4×10^3 cells/well) overnight. Then, cells were cultured with medium containing various amounts of empty FA-PEG-PLGA/PK3, FA-PEG-PLGA nanoparticles (defined as FA-PPNPs, FA-PNPs), siRNA loading FA-PEG-PLGA/PK3, FA-PEG-PLGA nanoparticles (defined as FA-siRNA-PPNPs, FA-siRNA-PNPs), or naked siRNA at a concentration of 100 nM siRNA. After 48 hr., to each well was added 20 μL of MTT and the plate was incubated for 4 hr. 150 μL of dimethyl sulfoxide was added into each well and the absorbance at 490 nm was measured. The cell viability was calculated as the formula below.

$$\textit{Cell viability} = \frac{\textit{Asample}-\textit{Ablank}}{\textit{Anegative control}-\textit{Ablank}}$$

Western blotting

Activated RAW 264.7 cells were incubated in a 6-well plate (2×10^5cell/well) and treated with naked siRNA, FA-siRNA-PNPs, or FA-siRNA-PPNPs containing an equal amount of siRNA (100 nM). Meanwhile, non-treated cells were used as control. After 48 hr., cells were lysed using RIPA buffer (containing 2% PMSF and 1% protease inhibitor cocktail). Total protein in the lysate was quantified using the bicinchoninic acid method and diluted to the same concentration with RIPA buffer.

The same amount of protein (40 μg) was separated on a 12% SDS-PAGE gel and transferred to polyvinylidene difluoride (PVDF) membranes (0.45 μm, Merck Millipore, Billerica, MA, USA) at 100 V for 2 hr. The PVDF membranes were blocked with 5% (w/v) bovine serum albumin with 0.1% (v/v) Tween 20 for 4 hr. at 4 °C and then incubated in primary antibodies for Mcl-1 or β-actin overnight at 4 °C. Then, PVDF membranes were incubated with horseradish peroxidase-conjugated secondary antibodies for 4 hr. at 4 °C. The membranes were transferred to work solution of ECL kit for 3 min and analyzed on a Bio Spectrum 600 imaging system from UVP company (Upland, CA, USA).

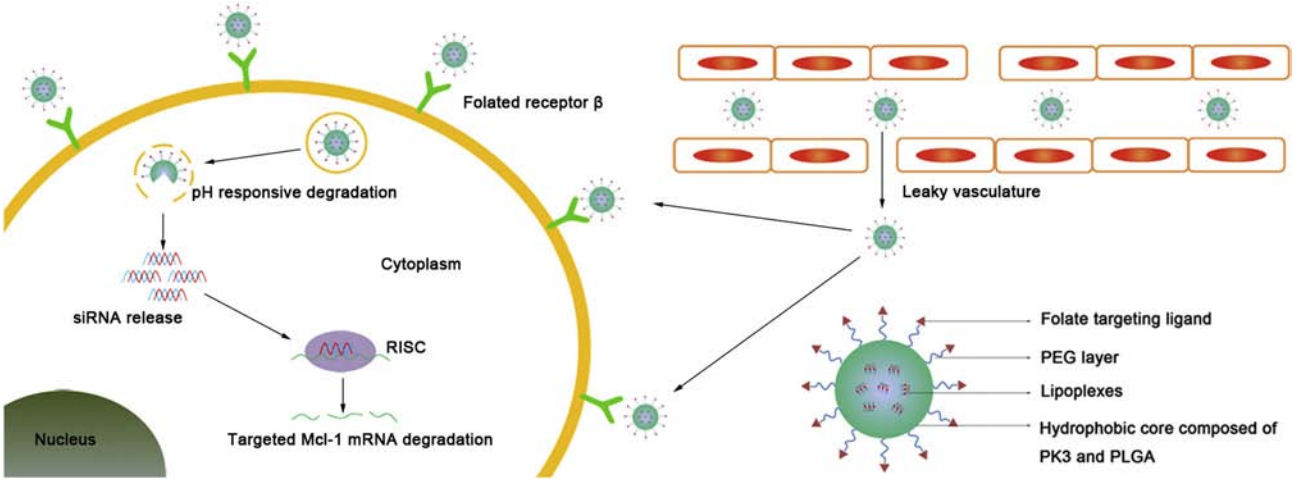

Figure 1. Schematic illustration of FA-siRNA-PPNPs delivery in AIA rats.

Establishment of an AIA rat model

Male Sprague Dawley rats (150–170 g each) were obtained from the Experimental Animal Center of Jilin University (Changchun, China) (license no. SCXK-(LIAO) 2015–0001). All animal experiments were performed according to the Institution of Animal Ethics Committee at Jilin University. 50 μL of Freund's complete adjuvant (10 mg/mL) was injected into the left hind footpad to induce AIA in the rat model.

In vivo biodistribution of siRNA delivered by FA-siRNA-PPNPs

AIA rats were used for investigating the biodistribution of siRNA delivered by FA-siRNA-PPNPs *in vivo*. Rats were injected with FA-siRNA-PPNPs containing Cy5-siRNA (4 nmol/kg) *via* the caudal vein. The same amount of naked siRNA (4 nmol/kg) was injected as a negative control. Four hr. after intravenous injection, the fluorescence of major tissues was photographed with IVIS Live Imaging System 100 from Xenogen Corp. (Alameda, CA, USA).

In vivo RA therapy

AIA rat model was established for *in vivo* RA therapy (Figure 1). After 14 days, the rats were randomly divided into five groups (n = 6) and injected with naked siRNA, FA-siRNA-PNPs, or FA-siRNA-PPNPs in saline at an siRNA dosage of 4 nmol/kg *via* caudal vein every 2 days for three times. Normal and AIA rats injected with the same volume of saline were also investigated as negative control and vehicle control groups. Clinical score of AIA rats were graded as follow: 0 (normal), 1 (slight swelling and confined erythema), 2 (slight swelling and extended erythema), 3 (moderate swelling and extended erythema), and 4 (severe swelling and widespread erythema).[35] On day 20, the paw thickness was measured by an electrical Vernier caliper.

Biochemical analysis of serum and histological analysis

Rats were sacrificed 20 days after AIA induction. Serum and ankle joints of all rats were collected. Serum levels of tumor necrosis factor (TNF-α), interleukin-6 (IL-6), and interleukin-1β (IL-1β) were determined by ELISA kits from Elabscience Biotechnology, (Wuhan, China) for cytokine evaluation.

For histological analysis, the ankle joints were stained with Hematoxylin and Eosin (H&E). Briefly, the ankle joints were fixed in 4% (w/v) phosphate-buffered paraformaldehyde for 24 hr., decalcified in 10% (w/v) EDTA solution for four weeks, embedded in paraffin, and sectioned (5 μm). The slices were photographed using an Olympus CKX41 inverted fluorescent microscope from (Tokyo, Japan).

Statistical analysis

The statistical significance of differences among the groups tested was determined using one-way ANOVA. Data are expressed as mean ± SD. $P < 0.05$ was considered statistically significant.

Results

Preparation of FA-siRNA-PPNPs

For the preparation of FA-siRNA-PPNPs, Mcl-1 siRNA-DOTAP lipoplexes were initially formed. Then, the Mcl-1 siRNA-DOTAP lipoplexes were encapsulated into pH-sensitive material PK3 and FA-PEG-PLGA for the targeting of FRβ overexpressed by activated macrophages through an emulsion–solvent evaporation method. A series of PPNPs with varying compositions were investigated to optimize particle size, as shown in Table 1. When the ratio of PK3-to-PLGA changed from 10:0 to 2:8 (Batch 1–6), the particle size changed from 163.1 ± 1.37 nm to 197 ± 4.29 nm. When the ratio of PK3-to-PLGA was 5:5 (Batch 4), the nanoparticles had the smallest size and PDI (163.1 ± 1.37 nm, 0.134 ± 0.017). Subsequently, the ratio of PLGA-to-FA-PEG-PLGA used was optimized. As shown in Batch 8–13, with the increase of FA-PEG-PLGA, the particle size decreased. When the ratio of PLGA-to-FA-PEG-PLGA was 0:10 (Batch 13), nanoparticles had the smallest size

Table 1
Compositions and characteristics of PNP formulations.

Batch	PK3:PLGA(w:w)	FA-PEG-PLGA:PLGA (w:w)	Size (nm)	PDI	Zeta potential (mV)
1	10:0	0:10	197 ± 4.29	0.124 ± 0.033	8.3 ± 0.56
2	8:2	0:10	182.4 ± 5.55	0.145 ± 0.008	6.7 ± 0.72
3	6:4	0:10	174.7 ± 5.46	0.141 ± 0.006	5.0 ± 0.49
4	5:5	0:10	163.1 ± 1.37	0.134 ± 0.017	4.8 ± 0.39
5	4:6	0:10	172.6 ± 3.84	0.137 ± 0.017	4.5 ± 0.27
6	2:8	0:10	177.1 ± 5.88	0.189 ± 0.020	3.1 ± 0.61
7	0:10	0:10	192.9 ± 7.48	0.135 ± 0.019	2.1 ± 0.38
8	5:5	2:8	170.3 ± 8.82	0.130 ± 0.021	4.6 ± 0.53
9	5:5	4:6	164.5 ± 2.69	0.166 ± 0.018	4.2 ± 0.35
10	5:5	5:5	159 ± 5.07	0.145 ± 0.024	4.0 ± 0.28
11	5:5	6:4	153.4 ± 2.32	0.171 ± 0.035	4.2 ± 0.32
12	5:5	8:2	148.4 ± 2.25	0.138 ± 0.017	3.9 ± 0.42
13	5:5	10:0	142.6 ± 0.61	0.112 ± 0.020	3.6 ± 0.43

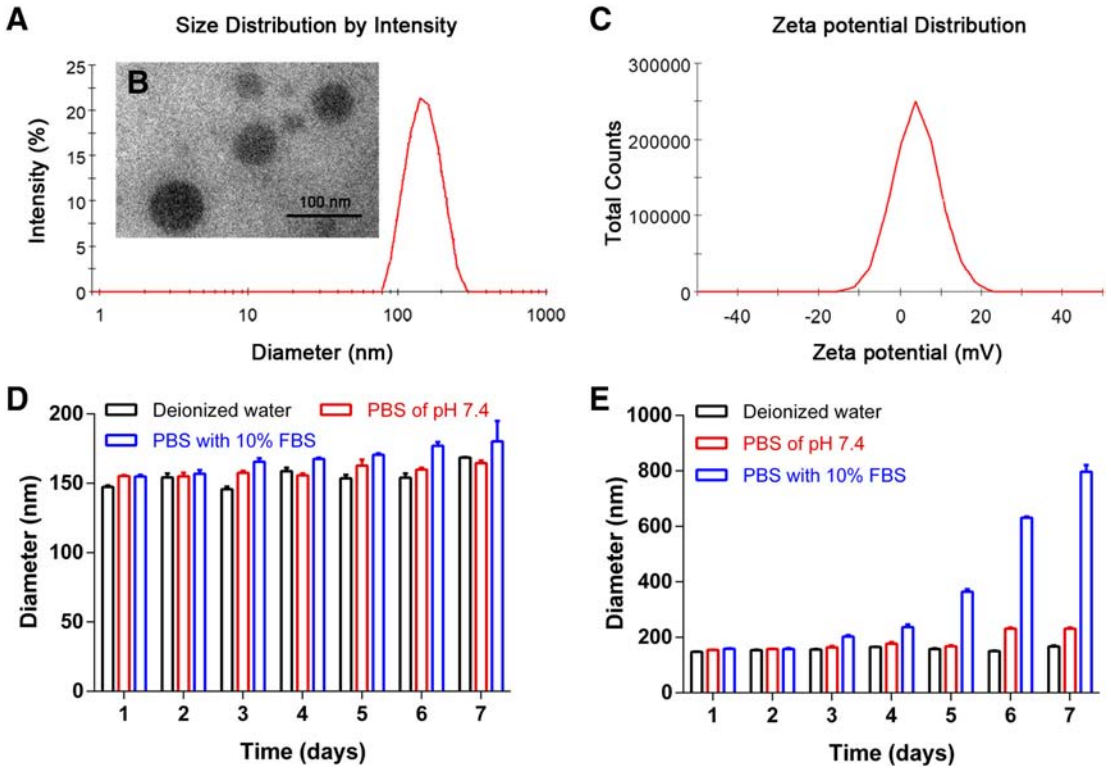

Figure2. Characteristics of FA-siRNA-PPNPs. (A) Size distribution of FA-siRNA-PPNPs. (B) The TEM image of FA-siRNA-PPNPs. (C) Zeta potential distribution of FA-siRNA-PPNPs. (D) *In vitro* stability of FA-siRNA-PPNPs in different mediums at 4 °C and (E) at 37 °C. Values are mean ± SD (n = 3).

and PDI (142.6 ± 0.61 nm, 0.112 ± 0.02), and, therefore, Batch 13 was the optimized formulation.

Characterization of FA-siRNA-PPNPs

The average size of FA-siRNA-PPNPs was 142.6 ± 0.61 nm, while PDI was 0.112 ± 0.02 indicating a narrow size distribution (Figure 2, *A* and Table 1). FA-siRNA-PPNPs had a zeta potential of 3.6 ± 0.43 mV (Figure 2, *C* and Table 1). The size and morphology of FA-siRNA-PPNPs were observed under TEM. As shown in Figure 2, *B*, FA-siRNA-PPNPs formed a smooth spherical structure with a size of approximately 100 nm. The percentage of siRNA loading and encapsulation efficiency of siRNA for FA-siRNA-PPNPs was 0.081 ± 0.007% and 62.4 ± 5.4%, respectively.

Stability of FA-siRNA-PPNPs

To evaluate the stability of FA-siRNA-PPNPs, particle size, zeta potential, encapsulation efficiency and morphology of FA-siRNA-PPNPs were investigated at both 4 °C and 37 °C in different media. The particle size and zeta potential of FA-

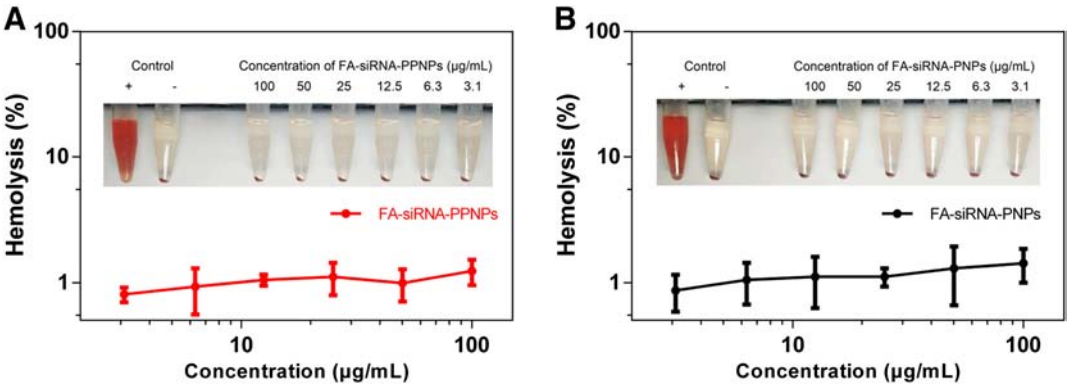

Figure 3. Hemolysis of induction of nanoparticles. Red blood cells were treated with (A) FA-siRNA-PPNPs solution and (B) FA-siRNA-PNPs solution. Values are mean ± SD (n = 6).

siRNA-PPNPs showed no significant change in different media at 4 °C in 7 days, indicating that nanoparticles were stable at 4 °C (Figure 2, *D* and S1, *A*). FA-siRNA-PPNPs also retained its spherical shape in deionized water at 4 °C (Figure S1, *C*). As shown in Figure S1, *C* and *D*, the encapsulation efficiency of FA-siRNA-PPNPs changed from 62.1 ± 3.2% to 58.7 ± 2.3% after 7 days in deionized water. However, the encapsulation efficiency of FA-siRNA-PPNPs was 50.4 ± 3.1% to 57.2 ± 3.3% after 1 day in deionized water at 37 °C, PBS and PBS with 10% FBS at both 4 °C and 37 °C. These results suggested that FA-siRNA-PPNPs were stable in deionized water at 4 °C.

As shown in Figure 2, *E*, however, there was a significant size change in the nanoparticles after 3 days in PBS with 10% FBS and also a significant change after 6 days in PBS at 37 °C, which indicated particle aggregation. An irregular spherical shape of FA-siRNA-PPNPs was also observed by TEM after 7 days in PBS and PBS with 10% FBS at 37 °C (Figure S2, *E* and *F*). As shown in Figure S2, *F*, FA-siRNA-PPNPs showed a significant increase in particle size, which was consistent with the results of particle size. These results suggested that FA-siRNA-PPNPs could be stable *in vivo* for at least 2 days and are suitable for system administration.

Hemolysis tests

The hemolysis rate of FA-siRNA-PPNPs and FA-siRNA-PNPs were both below 5% at a concentration of nanoparticles from 3.1 to 100 μg/mL (Figure 3). It was suggested that both FA-siRNA-PPNPs and FA-siRNA-PNPs had good biocompatibility and safety for intravenous injection

In vitro release

The *in vitro* release of FA-siRNA-PPNPs containing Cy5-labeled siRNA was performed in PBS (10 mM, pH 7.4 and pH 5.0) (Figure 4). FA-siRNA-PPNPs showed burst release at both pH 7.4 (17%) and pH 5.0 (42%) within 1 hr. The release of siRNA at pH 7.4 reached a plateau with a release of 43% for 6 hr. However, the cumulative release of siRNA encapsulated in FA-siRNA-PPNPs reached about 71% at pH 5.0 within 6 hr. The higher release of siRNA at pH 5.0 for 24 hr. revealed a pH-sensitive property of FA-siRNA-PPNPs. These results indicated that the encapsulated siRNA was rapidly released from FA-siRNA-PPNPs at an acidic pH, allowing for efficient delivery to the targeted inflammation tissues.

Cell-uptake studies

The cell uptake of FA-siRNA-PPNPs and FA-siRNA-PNPs loaded with Cy5-siRNA was determined in activated RAW 264.7 cells. The mean fluorescence intensity of cells treated with FA-siRNA-PPNPs and FA-siRNA-PNPs was significantly higher than those treated with naked siRNA ($P < 0.001$) (Figure 5, *A*). These results suggest FR-mediated cellular uptake of siRNA. The mean fluorescence intensity of cells treated with FA-siRNA-PPNPs was significantly higher than those treated with FA-siRNA-PNPs ($P < 0.01$) (Figure 5, *A*), which indicated that FA-siRNA-PPNPs had higher cellular uptake of siRNA than that of FA-siRNA-PNPs.

The intracellular distribution of nanoparticles containing Cy5-siRNA was investigated by CLSM in activated RAW 264.7 cells. As shown in Figure 5, *B*, red fluorescence from Cy5-siRNA was observed in the cytoplasm and near the nucleus, which indicated that siRNA was released into the cytoplasm. Moreover, the fluorescence intensity of FA-siRNA-PPNPs treated cells was higher than that of FA-siRNA-PNPs, consistent with the results of flow cytometry. These results indicated that the rapid release of siRNA from FA-siRNA-PPNPs occurred owing to their degradation in acidic intercellular microenvironment contributing to stronger fluorescence intensity.

Cytotoxicity assays

The cytotoxicity of FA-PPNPs and FA-PNPs was evaluated by MTT assay. There was no significant cytotoxicity for either empty FA-PPNPs or FA-PNPs (Figure 5, *C*).

As shown in Figure 5, *D*, naked siRNA showed no significant cytotoxicity against untreated activated RAW 264.7 cells. Meanwhile, FA-siRNA-PPNPs and FA-siRNA-PNPs exhibited significant cytotoxicity. Moreover, FA-siRNA-PPNPs had higher cytotoxicity than FA-siRNA-PNPs. This is likely because that, compared with FA-siRNA-PNPs, the pH-sensitive nanoparticle FA-siRNA-PPNPs could rapidly release Mcl-1 siRNA in activated macrophages and resulted in enhanced cytotoxicity.

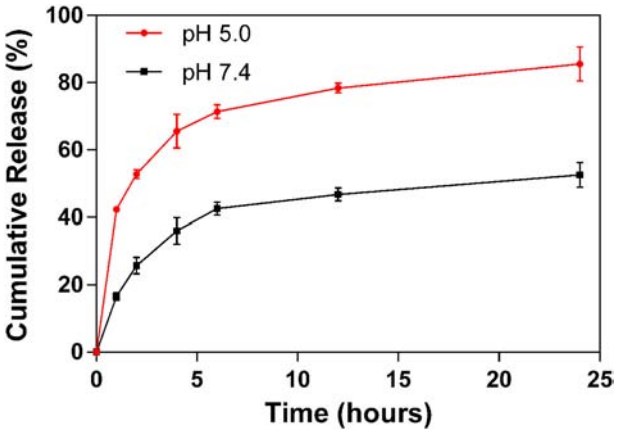

Figure 4. *In vitro* siRNA release from FA-siRNA-PPNPs at pH 5.0 and pH 7.4 at 37 °C. Values are mean ± SD (n = 3).

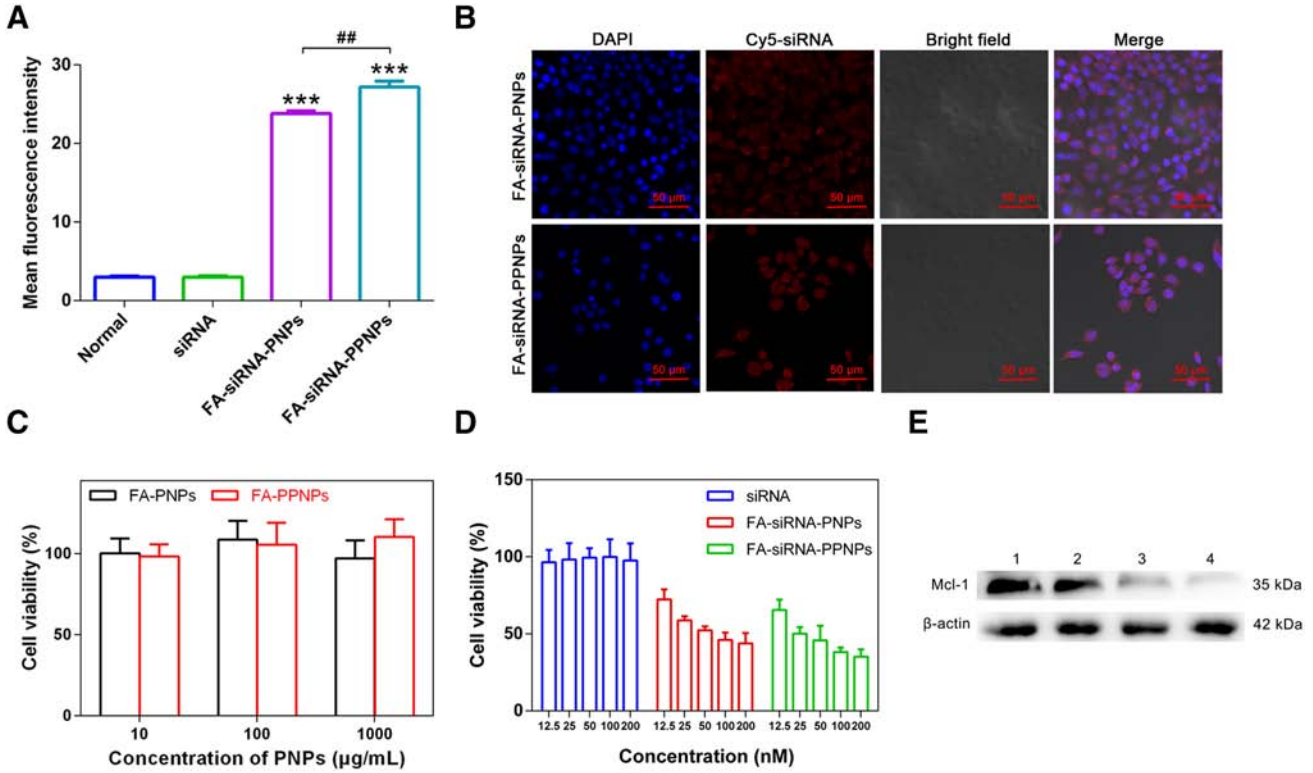

Figure 5. Uptake and bioactivity of siRNA nanoparticles in RAW 264.7 cells. (A) Flow cytometry. ***$P < 0.001$ represents FA-siRNA-PNPs or FA-siRNA-PPNPs *versus* siRNA, $^{\#\#}P < 0.01$. Values are mean ± SD (n = 3). (B) Confocal microscopy. (C) Cytotoxicity of blank FA-PNPs and FA-PPNPs. Values are mean ± SD (n = 6). (D) Cytotoxicity of naked siRNA, FA-siRNA-PNPs, and FA-siRNA-PPNPs. Values are mean ± SD (n = 6). (E) Mcl-1 protein in activated RAW 264.7 cells analyzed by Western blot. Rank 1: Control, rank 2: naked siRNA, rank 3: FA-siRNA-PNPs, and rank 4: FA-siRNA-PPNPs.

Western blotting

To demonstrate the effects of FA-siRNA-PPNPs and FA-siRNA-PNPs on the expression levels of Mcl-1 protein, western blotting was applied. The expression levels of Mcl-1 protein treated with FA-siRNA-PPNPs and FA-siRNA-PNPs were lower than those treated by naked siRNA or control (Figure 5, *E*). The Mcl-1 protein expression level of cells treated with FA-siRNA-PPNPs was the lowest. These results indicated that FA-siRNA-PPNPs significantly reduced the expression level of Mcl-1 protein in the activated macrophages.

Biodistribution of FA-siRNA-PPNPs in vivo

To evaluate the delivery and distribution of siRNA *in vivo*, naked siRNA and FA-siRNA-PPNPs were i.v. injected and

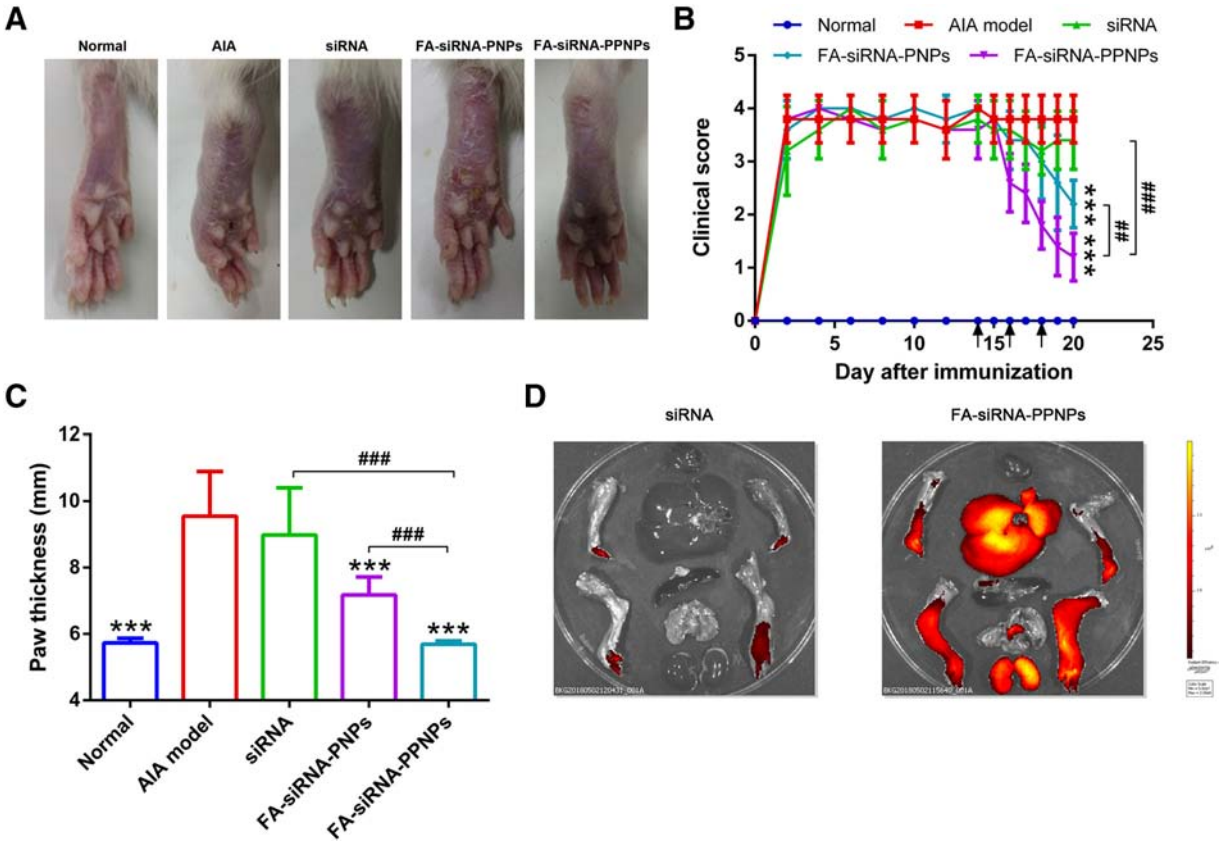

Figure 6. Therapeutic efficacy and tissue distribution in AIA rats. (A) Photographs of rat paws. (B) Mean clinical score after immunization (arrow represents different formulations treatment) Values are mean ± SD (n = 5, ***$P < 0.001$ *versus* AIA model, $^{\#\#}P < 0.01$, $^{\#\#\#}P < 0.001$). (C) Paw thickness. Values are mean ± SD (n = 5, ***$P < 0.001$ *versus* AIA model, $^{\#\#\#}P < 0.001$). (D) Tissue distribution of Cy5-siRNA and FA-siRNA-PPNPs in AIA rats.

fluorescence imaging of major tissues performed at four hours after injection. (Figure 6, *D*) FA-siRNA-PPNPs treated AIA rats showed stronger fluorescence intensity in the ankle joints, which indicated FR-mediated uptake of nanoparticles. In contrast, the fluorescence signal was barely detected in major tissues of naked siRNA treated AIA rats, which could be due to rapid degradation of the siRNA by nucleases in the blood and renal clearance. These results indicated that the nanoparticles protected the encapsulated siRNA from serum nucleases and prolonged its blood circulation time.

The therapeutic effect of FA-siRNA-PPNPs on AIA rats

AIA was established in a rat model to evaluate the therapeutic efficacy of FA-siRNA-PPNPs in RA. The rats were then treated every other day with saline, naked siRNA, FA-siRNA-PNPs, or FA-siRNA-PPNPs. Untreated normal rats were included as a control. Photographs of hind paws of saline-treated AIA rats and naked siRNA treated AIA rats showed significant swelling and erythema, compared with normal rats. FA-siRNA-PPNPs treated AIA rats exhibited the least amount of swelling and erythema (Figure 6, *A*). Figure 6, *B* showed the mean clinical score of rats in different groups. The mean clinical score of saline-treated AIA rats was 3.8, and that of naked siRNA treated rats was 3.4. Twenty days after induction of AIA, which indicated no significant difference. However, the mean clinical score of FA-siRNA-PPNPs treated AIA rats with showed a marked decrease compared with saline, naked siRNA and FA-siRNA-PNPs treated rats ($P < 0.001$, $P < 0.001$, and $P < 0.01$, respectively). Paw thickness was measured after the treatment. Paw thickness of FA-siRNA-PPNPs and FA-siRNA-PNPs treated AIA rats was thinner than those of saline or naked siRNA treated AIA rats ($P < 0.001$). Moreover, rats treated with FA-siRNA-PPNPs significantly reduced paw thickness compared with saline, naked siRNA or FA-siRNA-PNPs treated AIA rats ($P < 0.001$). These results indicated that FA-siRNA-PPNPs significantly improved the clinical outcomes in AIA rats.

Pro-inflammatory cytokines were associated with inflammation and joint destruction in RA. Serum levels of pro-inflammatory cytokines (TNF-α, IL-6, and IL-1β) in AIA rats were determined (Figure 7, *A*). The levels of pro-inflammatory cytokines were significantly elevated in the serum of saline-treated rats, compared with normal rats ($P < 0.001$). As expected, the levels of pro-inflammatory cytokines in naked siRNA-treated rats were not significantly decreased, compared with a saline-treated rat. However, the levels of pro-inflammatory cytokines were decreased significantly in FA-siRNA-PPNPs or FA-siRNA-PNPs treated AIA rats. Moreover, the FA-siRNA-PPNPs treated AIA rats exhibited a lower level of pro-inflammatory cytokines than that of FA-siRNA-PNPs treated AIA rats ($P < 0.05$).

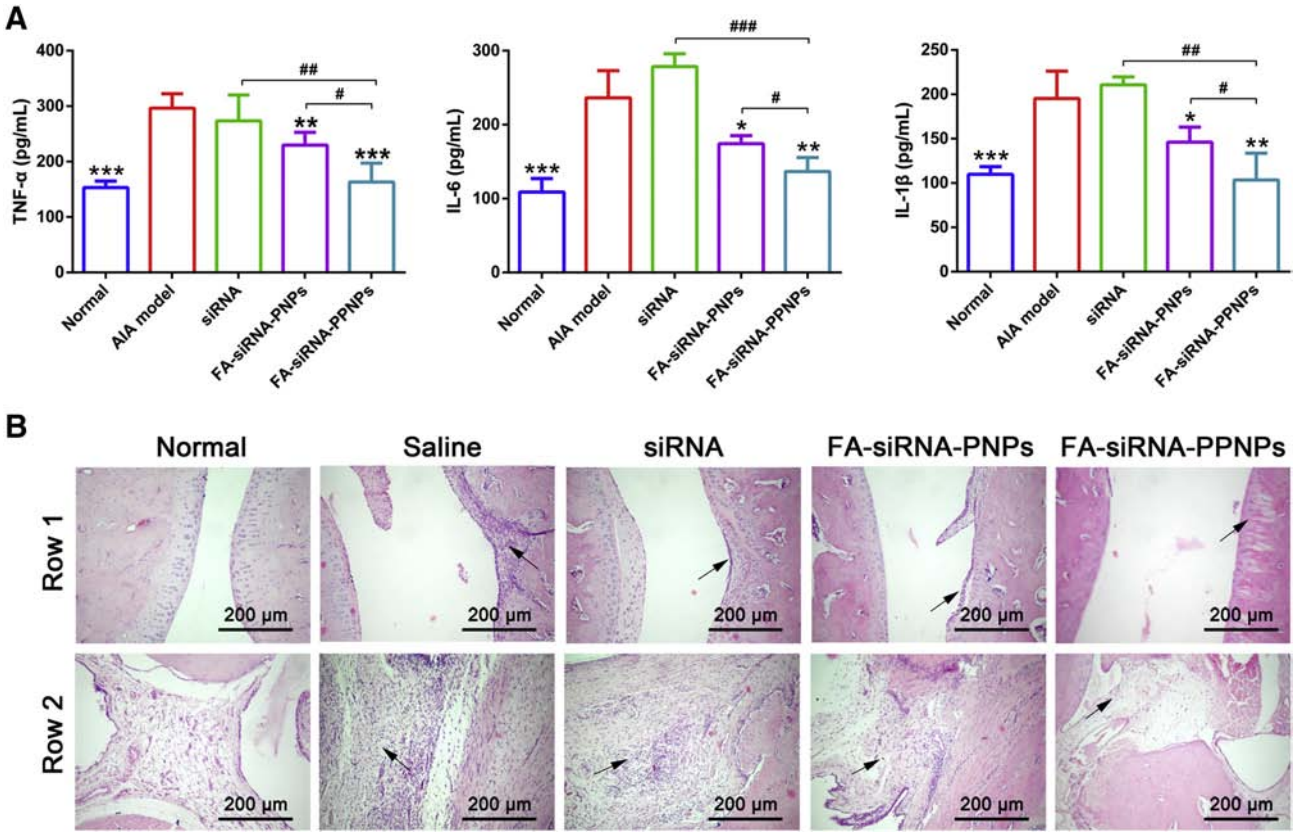

Figure 7. Effects of treatment on cytokine induction and joint tissues. (A) Cytokine levels in serum of AIA rats treated with saline, naked siRNA, FA-siRNA-PNPs or FA-siRNA-PPNPs. Values are mean ± SD (n = 5, $^{*}P < 0.05$, $^{**}P < 0.01$, $^{***}P < 0.001$ *versus* AIA model, $^{\#}P < 0.05$, $^{\#\#}P < 0.01$, $^{\#\#\#}P < 0.001$). (B) In (Row 1) and around (Row 2) ankle joints treated with various formulations were histologically evaluated after H&E staining (original magnification ×100).

For further evaluation of therapeutic effect in AIA rats, ankle joints were sectioned and stained by H&E for histological analysis (Figure 7, *B*). Saline and naked siRNA treated AIA rats demonstrated severe fibroplasia and infiltration of inflammatory cells in and around the ankle joints. In contrast, FA-siRNA-PNPs treated AIA rats demonstrated decreased fibroplasia and infiltration of inflammatory cells in and around ankle joints, compared with saline-treated AIA rats. Furthermore, FA-siRNA-PPNPs treated AIA rats demonstrated no fibroplasia and only mild infiltration of inflammatory cells in and around the ankle joints.

Discussion

Mcl-1, an anti-apoptotic protein, is a potential therapeutic target in RA.[17,18] Mcl-1 siRNA could specifically silence the expression of Mcl-1 protein, which may induce apoptotic cell death and provide an effective treatment of RA. However, because of poor delivery efficiency, the clinical application of siRNA has been limited.[36] Therefore, it is crucial to develop a safe and efficient delivery system for siRNA therapy. PNPs are promising for siRNA delivery. They protect siRNA from the degradation by nuclease and prolong its circulation time in blood.[37] PNPs are designed to be stable in serum and to release in endosomes in a timely manner.[38] Due to the acidic pH in inflammation (~6.5), endosomes (5.5–6.5), and lysosomes (4.5–5.0), pH-sensitive polymers have been exploited for drug delivery in inflammatory diseases treatment.[39,40] Previous studies have shown that biocompatibility and biodegradability of a pH-sensitive drug delivery system are important.[41] PK3, a novel polyketal, is stable at neutral or alkaline pH and has a short hydrolysis half-time at pH 4.5, with neutral biocompatible degradation products. It is an excellent material for constructing drug carriers for drug delivery to inflammation tissues.[32]

In this study, we successfully constructed pH-sensitive and FR-targeting nanoparticles (FA-siRNA-PPNPs) to deliver Mcl-1 siRNA comprised of FR-targeting ligands, a PEG shell, a pH-sensitive hydrophobic polymeric core, and DOTAP/siRNA lipoplexes encapsulated in the polymeric core. The PEG shell of FA-siRNA-PPNPs helped in the escape from the reticular endothelial system. The FA-siRNA-PPNPs had a size of 142.6 ± 0.61 nm and a narrow PDI of 0.112 ± 0.02 (Figure 2, *A* and Table 1), which was suitable for accumulation in inflammation tissues by the ELVIS mechanism. The FR-targeting ligands on the surface of FA-siRNA-PPNPs endowed the particles with high affinity for FRβ on macrophages. Importantly, the pH-sensitive polymeric core of FA-siRNA-PPNPs was designed to facilitate the intracellular release of Mcl-1 siRNA. The zeta potential of FA-siRNA-PPNPs was 3.6 ± 0.43 mV. Moreover, FA-siRNA-PPNPs

had a smooth spherical structure under TEM (Figure 2, *B*), along with a high encapsulation efficiency of 62.4 ± 5.4%.

Stability and biocompatibility are important for the storage and application of nanoparticles. The stability of FA-siRNA-PPNPs was evaluated in deionized water, PBS, and PBS containing 10% FBS, which represented the storage, *in vitro*, and *in vivo* condition, respectively. Our results demonstrated that FA-siRNA-PPNPs had good storage and *in vitro* stability. FA-siRNA-PPNPs had serum stability of 2 days, which was enough for *in vivo* distribution of nanoparticles after administration. Hemolysis tests have demonstrated that FA-siRNA-PPNPs and FA-siRNA-PNPs had good biocompatibility (Figure 3). To evaluate the biocompatibility of unloaded siRNA nanoparticles with activated RAW 264.7 cells, the cytotoxicity experiments of FA-PPNPs and FA-PNPs were also carried out. As shown in Figure 5, *D*, FA-PPNPs and FA-PNPs had no significant cytotoxicity suggesting a lack of vehicle-related effect.

The *in vitro* release behavior of FA-siRNA-PPNPs was performed in acidic (pH 5.0) and neutral (pH 7.4) environments. As expected, the release of Mcl-1 siRNA was pH-dependent. We then investigated the siRNA delivery efficiency *in vitro*. The cellular uptake of FA-siRNA-PPNPs was more efficient compared with FA-siRNA-PNPs, which was due to its faster degradation in the acidic intercellular microenvironment (Figure 5, *A* and *B*). Our results suggested that FA-siRNA-PPNPs exhibited significant cytotoxicity and downregulated expression level of Mcl-1 protein to activated RAW 264.7 cells. The faster degradation of FA-siRNA-PPNPs in cells contributed to the higher intercellular accumulation of siRNA and resulted in enhanced cytotoxicity, consistent with cellular uptake results. These results indicated that FA-siRNA-PPNPs was an efficient carrier for siRNA delivery.

Biodistribution study showed that FA-siRNA-PPNPs targeted inflamed ankle joints and prolonged blood circulation time.

Finally, we examined the therapeutic effects of FA-siRNA-PPNPs in an AIA rat model for RA. FA-siRNA-PPNPs treatment led to a significant improvement in the clinical outcomes of paws (Figure 6, *A–C*). The lower level of pro-inflammatory cytokines confirmed the inflammation inhibition of FA-siRNA-PPNPs (Figure 7, *A*). Moreover, severe fibroplasia and infiltration of inflammatory cells were shown in saline and naked siRNA treated AIA rats, however, FA-siRNA-PPNPs treated AIA rats showed no fibroplasia and mild infiltration of inflammatory cells. Overall, these results indicated the significant therapeutic effects of FA-siRNA-PPNPs with AIA rats.

In conclusion, functional polymeric nanoparticles FA-siRNA-PPNPs based on PK3 and FA-PEG-PLGA were developed for the treatment of RA. FA-siRNA-PPNPs showed accelerated siRNA release in acidic pH, which indicated its pH-sensitivity. The increased delivery of siRNA to the target inflammation tissue showed the FR-targeting property of FA-siRNA-PPNPs. Moreover, FA-siRNA-PPNPs was effective in the treatment of RA in an AIA rat model. Therefore, FA-siRNA-PPNPs have been shown to be a promising siRNA delivery platform for inflammation therapy.

Acknowledgements

This study was supported by Jilin Province Science and Technology Development Program (No.20180101269JC).

Appendix A. Supplementary data

Supplementary data to this article can be found online at https://doi.org/10.1016/j.nano.2019.102017.

References

1. Feldmann M. Pathogenesis of arthritis: recent research progress. *Nat Immunol* 2001;**2**:771-3.
2. Abbasi M, Mousavi MJ, Jamalzehi S, Alimohammadi R, Bezvan MH, Mohammadi H, et al. Strategies toward rheumatoid arthritis therapy; the old and the new. *J Cell Physiol* 2019;**234**:10018-31.
3. McCarberg BH, Cryer B. Evolving therapeutic strategies to improve nonsteroidal anti-inflammatory drug safety. *Ther* 2015;**22**:e167-78.
4. Petta I, Peene I, Elewaut D, Vereecke L, De Bosscher K. Risks and benefits of corticosteroids in arthritic diseases in the clinic. *Biochem Pharmacol* 2019.
5. Chiba T, Sato K, Endo M, Ando T, Inomata M, Orii S, et al. Upper gastrointestinal disorders induced by non-steroidal anti-inflammatory drugs. *Hepato-Gastroenterology* 2005;**52**:1134-8.
6. Lorenz HM, Kalden JR. Perspectives for TNF-alpha-targeting therapies. *Arthritis Res Ther* 2002;**4**:S17-24.
7. Finckh A, Simard JF, Gabay C, Guerne PA, Phys S. Evidence for differential acquired drug resistance to anti-tumour necrosis factor agents in rheumatoid arthritis. *Ann Rheum Dis* 2006;**65**:746-52.
8. Lee DM, Weinblatt ME. Rheumatoid arthritis. *Lancet* 2001;**358**:903-11.
9. Gaffo A, Saag KG, Curtis JR. Treatment of rheumatoid arthritis. *Health Syst Pharm* 2006;**63**:2451-65.
10. Firestein GS. Immunologic mechanisms in the pathogenesis of rheumatoid arthritis. *J Clin Rheumatol* 2005;**11**:S39-44.
11. Davis BP, Ballas ZK. Biologic response modifiers: indications, implications, and insights. *J Allergy Clin Immunol* 2017;**139**:1445-56.
12. Kinne RW, Brauer R, Stuhlmuller B, Palombo-Kinne E, Burmester GR. Macrophages in rheumatoid arthritis. *Arthritis Res* 2000;**2**:189-202.
13. Mateen S, Zafar A, Moin S, Khan AQ, Zubair S. Understanding the role of cytokines in the pathogenesis of rheumatoid arthritis. *Clin Chim Acta* 2016;**455**:161-71.
14. Chu JG, Wang XJ, Bi HJ, Li LF, Ren MG, Wang JW. Dihydromyricetin relieves rheumatoid arthritis symptoms and suppresses expression of pro-inflammatory cytokines via the activation of Nrf2 pathway in rheumatoid arthritis model. *Int Immunopharmacol* 2018;**59**:174-80.
15. Yu RX, Yu RT, Liu Z. Inhibition of two gastric cancer cell lines induced by fucoxanthin involves downregulation of mcl-1 and STAT3. *Hum Cell* 2018;**31**:50-63.
16. Pope RM. Apoptosis as a therapeutic tool in rheumatoid arthritis. *Nat Rev Immunol* 2002;**2**:527-35.
17. Liu HT, Eksarko P, Temkin V, Haines GK, Perlman H, Koch AE, et al. Mcl-1 is essential for the survival of synovial fibroblasts in rheumatoid arthritis. *J Immunol* 2005;**175**:8337-45.
18. Liu HT, Huang QQ, Shi B, Eksarko P, Temkin V, Pope RM. Regulation of mcl-1 expression in rheumatoid arthritis synovial macrophages. *Arthritis Rheum* 2006;**54**:3174-81.
19. Leverson JD, Zhang H, Chen J, Tahir SK, Phillips DC, Xue J, et al. Potent and selective small-molecule MCL-1 inhibitors demonstrate on-target cancer cell killing activity as single agents and in combination with ABT-263 (navitoclax). *Cell Death Dis* 2015;**6**.
20. Nogueira E, Gomes AC, Preto A, Cavaco-Paulo A. Folate-targeted nanoparticles for rheumatoid arthritis therapy. *Nanomed Nanotechnol Biol Med* 2016;**12**:1113-26.
21. Mello CC, Conte D. Revealing the world of RNA interference. *Nature* 2004;**431**:338-42.
22. Courties G, Presumey J, Duroux-Richard I, Jorgensen C, Apparailly F. RNA interference-based gene therapy for successful treatment of rheumatoid arthritis. *Expert Opin Biol Ther* 2009;**9**:535-8.

23. Lee SJ, Son S, Yhee JY, Choi K, Kwon IC, Kim SH, et al. Structural modification of siRNA for efficient gene silencing. *Biotechnol Adv* 2013;**31**:491-503.
24. Kim WJ, Kim SW. Efficient siRNA delivery with non-viral polymeric vehicles. *Pharm Res* 2009;**26**:657-66.
25. Pecot CV, Calin GA, Coleman RL, Lopez-Berestein G, Sood AK. RNA interference in the clinic: challenges and future directions. *Nat Rev Cancer* 2011;**11**:59-67.
26. Wei X, Wu JB, Zhao G, Galdamez J, Lele SM, Wang XY, et al. Development of a Janus kinase inhibitor prodrug for the treatment of rheumatoid arthritis. *Mol Pharm* 2018;**15**:3456-67.
27. Wei X, Li F, Zhao G, Chhonker YS, Averill C, Galdamez J, et al. Pharmacokinetic and biodistribution studies of HPMA copolymer conjugates in an aseptic implant loosening mouse model. *Mol Pharm* 2017;**14**:1418-28.
28. Zhang YJ, Jia ZS, Yuan HJ, Dusad A, Ren K, Wei X, et al. The evaluation of therapeutic efficacy and safety profile of simvastatin prodrug micelles in a closed fracture mouse model. *Pharm Res* 2016;**33**:1959-71.
29. de Ilarduya CT, Sun Y, Duezguenes N. Gene delivery by lipoplexes and polyplexes. *Pharm Sci* 2010;**40**:159-70.
30. Lv HT, Zhang SB, Wang B, Cui SH, Yan J. Toxicity of cationic lipids and cationic polymers in gene delivery. *J Control Release* 2006;**114**:100-9.
31. Wang Y, Chang BS, Yang WL. pH-sensitive Polyketal nanoparticles for drug delivery. *J Nanosci Nanotechnol* 2012;**12**:8266-75.
32. Yang SC, Bhide M, Crispe IN, Pierce RH, Murthy N. Polyketal copolymers: a new acid-sensitive delivery vehicle for treating acute inflammatory diseases. *Bioconjug Chem* 2008;**19**:1164-9.
33. Cui ZR, Mumper RJ. Plasmid DNA-entrapped nanoparticles engineered from microemulsion precursors: in vitro and in vivo evaluation. *Bioconjug Chem* 2002;**13**:1319-27.
34. Ganta S, Devalapally H, Shahiwala A, Amiji M. A review of stimuli-responsive nanocarriers for drug and gene delivery. *J Control Release* 2008;**126**:187-204.
35. Heo R, Park JS, Jang HJ, Kim SH, Shin JM, Suh YD, et al. Hyaluronan nanoparticles bearing gamma-secretase inhibitor: in vivo therapeutic effects on rheumatoid arthritis. *J Control Release* 2014;**192**:295-300.
36. Wang J, Lu Z, Wientjes MG, Au JLS. Delivery of siRNA therapeutics: barriers and carriers. *AAPS J* 2010;**12**:492-503.
37. El-Say KM, El-Sawy HS. Polymeric nanoparticles: promising platform for drug delivery. *Pharm* 2017;**528**:675-91.
38. Hu Y, Zhao ZM, Ehrich M, Fuhrman K, Zhang CM. In vitro controlled release of antigen in dendritic cells using pH-sensitive liposome-polymeric hybrid nanoparticles. *Polymer* 2015;**80**:171-9.
39. Zhang J, Koh J, Lu JH, Thiel S, Leong BSH, Sethi S, et al. Local inflammation induces complement crosstalk which amplifies the antimicrobial response. *PLoS Pathog* 2009;**5**.
40. Zhang H, Xue YA, Huang J, Xia XY, Song MF, Wen KK, et al. Tailor-made magnetic nanocarriers with pH-induced charge reversal and pH-responsiveness to guide subcellular release of doxorubicin. *J Mater Sci* 2015;**50**:2429-42.
41. Liu J, Huang YR, Kumar A, Tan A, Jin SB, Mozhi A, et al. pH-sensitive nano-systems for drug delivery in cancer therapy. *Biotechnol Adv* 2014;**32**:693-710.